

RESEARCH ARTICLE | NOVEMBER 08 2024

Effects of lithographic and pattern parameters on stability of feature-edge location in electron beam lithography FREE

Special Collection: [Papers from the 67th International Conference on Electron, Ion and Photon Beam Technology and Nanofabrication \(EIPBN 2024\)](#)

Soo-Young Lee  

 Check for updates

J. Vac. Sci. Technol. B 42, 062604 (2024)

<https://doi.org/10.1116/6.0004017>



Articles You May Be Interested In

Analytic study of exposure contrast over feature edge in electron-beam lithography

J. Vac. Sci. Technol. B (December 2023)

Practical approach to modeling e-beam lithographic process from SEM images for minimization of line edge roughness and critical dimension error

J. Vac. Sci. Technol. B (December 2015)

3D modeling of electron-beam lithographic process from scanning electron microscope images

J. Vac. Sci. Technol. B (January 2021)



Instruments for Advanced Science



- Knowledge
- Experience
- Expertise

[Click to view our product catalogue](#)

Contact Hiden Analytical for further details:

www.HidenAnalytical.com
 info@hiden.co.uk



Gas Analysis

- ▶ dynamic measurement of reaction gas streams
- ▶ catalysis and thermal analysis
- ▶ molecular beam studies
- ▶ dissolved species probes
- ▶ fermentation, environmental and ecological studies



Surface Science

- ▶ UHV TPD
- ▶ SIMS
- ▶ end point detection in ion beam etch
- ▶ elemental imaging - surface mapping



Plasma Diagnostics

- ▶ plasma source characterization
- ▶ etch and deposition process reaction kinetic studies
- ▶ analysis of neutral and radical species



Vacuum Analysis

- ▶ partial pressure measurement and control of process gases
- ▶ reactive sputter process control
- ▶ vacuum diagnostics
- ▶ vacuum coating process monitoring

Effects of lithographic and pattern parameters on stability of feature-edge location in electron beam lithography

Cite as: J. Vac. Sci. Technol. B 42, 062604 (2024); doi: 10.1116/6.0004017

Submitted: 27 August 2024 · Accepted: 14 October 2024 ·

Published Online: 8 November 2024



Soo-Young Lee^{a)}

AFFILIATIONS

Department of Electrical and Computer Engineering, Auburn University, Auburn, Alabama 36849

Note: This paper is part of the Special Topic Collection: Papers from the 67th International Conference on Electron, Ion and Photon Beam Technology and Nanofabrication (EIPBN 2024).

^{a)}Author to whom correspondence should be addressed: leesoooy@auburn.edu

ABSTRACT

As the feature size continues to decrease, a high level of accuracy in achieving the feature boundary (“edge”) as designed becomes more essential. One of the reasons for any deviation in the feature-edge location is the proximity effect due to electron scattering in the resist. However, even with a perfect proximity effect correction (PEC), the nonideal process of resist development can still lead to a deviation in the edge location. In general, a higher exposure contrast over the feature edge leads to a smaller deviation in the edge location. In this study, an analytic model is employed in understanding the effects of the lithographic and pattern parameters on the deviation in the edge location due to the uncertainty in the lithographic process. Specifically, the closed-form mathematical expression of the deviation is derived in terms of the parameters that determine the exposure contrast. The results reported in this paper should be helpful in understanding better the deviation in the edge location without time-consuming repetitive simulation and developing a PEC method that enhances the stability of the feature boundaries in the written pattern, improving the process latitude.

Published under an exclusive license by the AVS. <https://doi.org/10.1116/6.0004017>

I. INTRODUCTION

Electron-beam (e-beam) lithography is widely used in writing a pattern of fine features on a substrate.^{1–5} The dimensional accuracy of written features is the most crucial metric of lithographic performance. The electron scattering in the resist during the process of exposing features often makes the size of a written feature deviate from the target dimension, i.e., the designed critical dimension (CD). This proximity effect has been a major issue in e-beam lithography, which puts a fundamental limit on the minimum feature size and pattern density that can be achieved. However, various methods of proximity effect correction (PEC) have been developed, which are successful in reducing the CD error significantly in many cases.^{6–10} Another issue that has not received much attention is the variation in CD due to the stochastic nature of the e-beam lithographic process. This stochastic variation is analyzed in this study. For clarity of presentation, the two terms, *dose* and *exposure*, are defined as follows.¹¹ The dose refers to the

energy (or amount of charge) given to a point on the surface of resist and the exposure the energy deposited at a point in the resist.

Uncertainty exists in the dose and exposure (especially the latter), the developing time, the concentration and spatial distribution of developer, etc., which makes the lithographic result stochastic. That is, even without the proximity effect, the size of a written feature may vary from location to location within a pattern and from experiment to experiment. This variation is to be minimized to produce consistent written patterns and achieve a high yield of working devices. The size of a feature is determined by its boundary consisting of edges. Fundamentally, the variation in edge location due to the randomness of the e-beam lithographic process needs to be minimized for writing a pattern with high consistency.

The outcome from the e-beam lithographic process heavily depends on the spatial distribution of exposure (“exposure distribution” hereafter) in a pattern. The exposure distribution in the edge region of a feature mostly determines where the feature edge would

11 November 2024 17:00:23

be after the development of resist. In particular, the exposure contrast over the feature edge has a direct effect on the stability of edge location. The higher the exposure contrast is, the smaller the variation in edge location due to the uncertainty in the e-beam lithographic process. The exposure contrast is affected by the lithographic and pattern parameters such as the electron-scattering ranges, the feature width, the reduction of feature width (often used for the PEC), etc. Hence, it is worthwhile to analyze the dependency of the stability of edge location on the parameters. A simulation approach to this analysis is very time-consuming since the simulation is computationally intensive and needs to be repeated for each individual case.

In a recent study,¹² an analytic approach, instead of simulation, was taken to the analysis of the exposure contrast. That is, the closed-form mathematical expressions of the exposure contrast have been derived in terms of the lithographic and pattern parameters. The expressions allow one to see the behaviors of the exposure contrast explicitly and avoid the time-consuming simulation. In this study, based on the analytic results of the exposure contrast, the stability of edge location is investigated analytically without resorting to simulation. Specifically, the deviation in the edge location caused by the stochastic lithographic process is derived in a closed-form expression with the double-Gaussian model of *line spread function* (LSF) and under the assumption that the exposure varies only in the lateral dimension and also linearly in the region close to the target edge. With the expression, one is able to analyze the effects of the lithographic and pattern parameters on the stability of feature edge easily without any simulation as will be demonstrated in this paper.

The significance of the results from this work includes the following: (1) They enable the fast analysis of the variation in edge location without simulation, (2) they may be used with both analytic and numeric forms of LSF, and (3) they can be utilized in developing a PEC scheme with an emphasis on the edge stability of written features.

The rest of the paper is organized as follows. The model for the analytic study is depicted in Sec. II. The exposure contrast and its analytic expression are briefly reviewed in Sec. III. The closed-form expression of the deviation in the edge location is derived in Sec. IV. Several examples of analyzing the stability of edge location using the expression are provided in Sec. V. The results and their validity and significance are summarized in Sec. VI.

II. ANALYTIC MODEL

The exposure distribution in the resist when a point is exposed with a unit dose is described by a point spread function (PSF). The double-Gaussian model of PSF is assumed though the outcomes from this study are still valid for other models of PSF, analytic or numeric.¹² Also, the exposure is assumed not to vary along the resist-depth dimension (note that the exposure variation with the depth is small for a thin resist or a high beam energy). Then, the PSF may be expressed as in Eq. (1),

$$psf(x, y) = \frac{1}{\pi(1 + \eta)} \left(\frac{1}{\alpha^2} e^{-\frac{x^2+y^2}{\alpha^2}} + \frac{\eta}{\beta^2} e^{-\frac{x^2+y^2}{\beta^2}} \right), \quad (1)$$

where α , β , and η are the forward-scattering and backscattering ranges and the ratio of the backscattered energy to the forward-scattered energy, respectively.

A vertically long rectangular feature with width W and length L illustrated in Fig. 1 is considered where X and Y axes correspond to the horizontal and vertical dimensions, respectively.

Suppose that the feature is exposed with a uniform dose D_0 . The exposure distribution cross the middle of the feature can be expressed as a function of x only,¹² $e(x)$, since the exposure does not vary with y when the feature is sufficiently long, i.e., $L \gg \beta$. That is,

$$e(x) = D_0 \int_0^W h(x - x') dx', \quad (2)$$

where $h(x)$ is the LSF that is defined as

$$h(x) = \int_{-\infty}^{\infty} psf(x, y) dy = \frac{1}{\sqrt{\pi}(1 + \eta)} \left(\frac{1}{\alpha} e^{-\frac{x^2}{\alpha^2}} + \frac{\eta}{\beta} e^{-\frac{x^2}{\beta^2}} \right). \quad (3)$$

The LSF, $h(x)$, in Eq. (3) describes the exposure distribution when a long line of points along the Y -axis is exposed with a uniform dose of 1. In this study where a long rectangular feature is considered, the LSF is employed instead of the PSF. Note that the LSF is equivalent to the 1D PSF.

In Fig. 2, the dose and exposure distributions, and the cross-section of the remaining resist profile, along the X -axis through the middle of a rectangular feature are illustrated. In the plot of exposure, the exposure contrast that is the slope of $e(x)$ at a point

11 November 2024 17:00:23

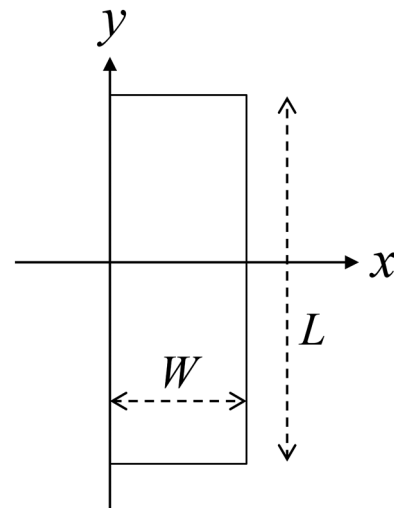


FIG. 1. Rectangular feature with width W and length L , which is long along the Y dimension.

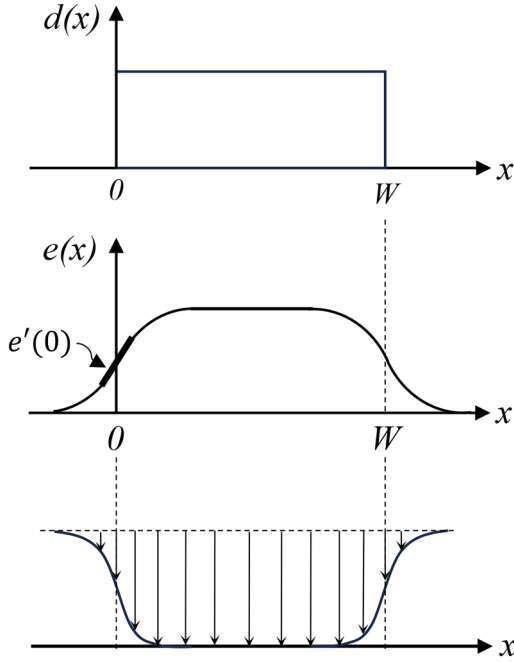


FIG. 2. Dose and exposure distributions and remaining resist profile of a rectangular feature with width W .

is also shown for $x = 0$. As indicated in the resist profile in Fig. 2, this study assumes that the resist is developed only in the vertical direction.

III. EXPOSURE CONTRAST

In this section, the previous study on the exposure contrast¹² is briefly reviewed for the case of a single feature to provide a basis for the investigation on the stability of edge location.

The exposure contrast is defined as the rate at which the exposure changes and may be quantified as the slope of the exposure curve $e(x)$ at x , i.e., $\frac{de(x)}{dx}$ or $e'(x)$ (see Fig. 2). In most cases, the exposure contrast is highest at the edge of an exposed region, not necessarily the target or designed edge. As discussed in the previous paper,¹² the location of the maximum exposure contrast is affected by the lithographic and pattern parameters.

For the proximity effect correction, the width of a long feature is often reduced by ΔW (where ΔW is to be optimized) on each side, $2\Delta W$ in total, i.e., the target width is W and the width to be exposed is $W - 2\Delta W$. Then, referring to Eq. (2), the exposure contrast $e'(x)$ can be computed as follows:

$$\begin{aligned} e'(x) &= \frac{de(x)}{dx} \\ &= D_0 \int_{\Delta W}^{W-\Delta W} \frac{dh(x-x')}{dx} dx' \\ &= D_0 [h(x-\Delta W) - h(x-W+\Delta W)]. \end{aligned} \quad (4)$$

For investigating the stability of edge location, the left target edge at $x = 0$ of rectangular feature (see Figs. 1 and 2) is considered in this paper, and hence, the exposure contrast $e'(0)$ is derived. By incorporating Eq. (3) into Eq. (4) for $x = 0$,

$$e'(0) = \frac{D_0}{\sqrt{\pi}(1+\eta)} \left[\frac{1}{\alpha} \left(e^{-\frac{\Delta W^2}{\alpha^2}} - e^{-\frac{(W-\Delta W)^2}{\alpha^2}} \right) + \frac{\eta}{\beta} \left(e^{-\frac{\Delta W^2}{\beta^2}} - e^{-\frac{(W-\Delta W)^2}{\beta^2}} \right) \right]. \quad (5)$$

Equation (5) explicitly shows the dependency of the exposure contrast on the lithographic (α , β , and η) and pattern (W and ΔW) parameters. The exposure contrast at the right target edge, $e'(W)$, can be derived similarly, which has the same absolute value but with the opposite sign as that at the left target edge. Note that the exposure contrast is positive at the left edge of a feature while negative at the right edge.

IV. STABILITY OF EDGE LOCATION

A. Developing rate

This study focuses on a small-scale deviation in the edge location due to the stochastic variation in the lithographic process, i.e., the edge region is the area of interest. The exposure distribution in the region close to the target edge ($x = 0$) may be modeled by a linear function of x as illustrated in Fig. 3, i.e.,

$$e(x) = k_e x + e_0, \quad (6)$$

where k_e is the slope of the linear function that is the exposure contrast at $x = 0$, i.e., $k_e = e'(0)$ [refer to Eq. (5)], and e_0 is the exposure level at $x = 0$, i.e., $e_0 = e(0)$.

From Eq. (2), $e(0)$ with the feature-width reduced by ΔW on each side can be derived as follows:

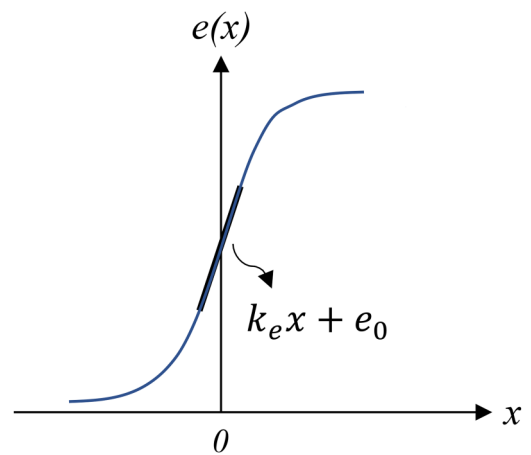


FIG. 3. Exposure distribution in the edge region may be modeled to be linear. The illustration is for the left edge at $x = 0$ of a feature.

11 November 2024 17:00:23

$$e(0) = D_0 \int_{\Delta W}^{W-\Delta W} h(-x') dx' = \frac{D_0}{\sqrt{\pi}(1+\eta)} \int_{\Delta W}^{W-\Delta W} \left(\frac{1}{\alpha} e^{-\frac{x'^2}{\alpha^2}} + \frac{\eta}{\beta} e^{-\frac{x'^2}{\beta^2}} \right) dx' \\ = \frac{D_0}{2(1+\eta)} \left[\operatorname{erf}\left(\frac{W-\Delta W}{\alpha}\right) - \operatorname{erf}\left(\frac{\Delta W}{\alpha}\right) + \eta \left(\operatorname{erf}\left(\frac{W-\Delta W}{\beta}\right) - \operatorname{erf}\left(\frac{\Delta W}{\beta}\right) \right) \right], \quad (7)$$

where $\operatorname{erf}()$ is the error function.

For the analysis not to be affected by the exposure level at the feature edge, only k_e is varied with e_0 fixed as illustrated in Fig. 4. For this purpose, the dose is adjusted such that e_0 is maintained at the same level [see Eq. (7)] as the parameters such as α are changed.

The developing rate of resist is a monotonically increasing function of the exposure where the function may be determined from experimental results.¹³ As the exposure increases, the developing rate increases slow in the region of low exposure, then increases rapidly, and finally levels out to its maximum for the exposure larger than a certain level (refer to the e -to- r mapping curve in Fig. 5). In the region of the rapid increase, the relationship between the exposure and developing rate can be approximated to be linear. Let k_{re} denote the slope of this linear part of the function. Then, the exposure can be mapped onto the developing rate as follows:

$$r(x) = k_{re}(e(x) - e_0) + r_0, \quad (8)$$

where r_0 corresponding to e_0 is the developing rate at the target edge.

In Fig. 5, the mapping of the exposure onto the developing rate is schematically shown where the distributions of exposure and developing rate are for the left edge at $x = 0$ of a feature. The distribution of the developing rate in terms of x can be obtained by incorporating the linear expression of $e(x)$ in Eq. (6) into Eq. (8),

$$r(x) = k_{re}k_e x + r_0 = k_r x + r_0, \quad (9)$$

where $k_r = k_{re}k_e$ is the contrast of developing rate over the feature edge at $x = 0$.

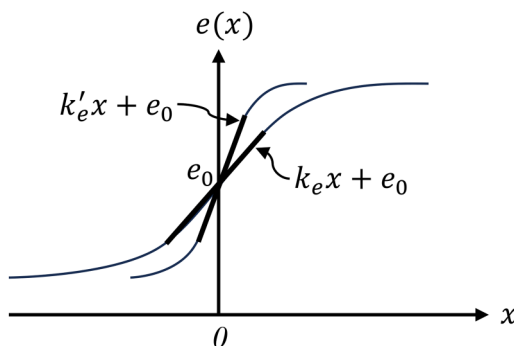


FIG. 4. Exposure level at the edge is fixed and only the exposure contrast is varied.

Since in the edge region, both the exposure-to-developing rate mapping and exposure are linear, the developing-rate distribution in the edge region is also linear as illustrated in Fig. 5.

B. Edge deviation

It is assumed in this study that the resist is developed only in the vertical direction from the top surface to the bottom of resist. The width of a feature after development is measured at the middle layer of resist (see Fig. 6). The developing time T_0 is set such that the resist is developed down to the middle layer at the target edge, i.e., $T_0 = \frac{H}{2r_0}$, where H is the thickness of the resist.

The variation (randomness) in developing time, exposure level, developer concentration, etc., can all cause the deviation in the edge location. Nevertheless, their effects are equivalent to each other. For example, the increased exposure level has the same effect on the edge location as the increased developing time, and a lower developer concentration is equivalent to the decreased developing time. Hence, in this study, only the uncertainty in the developing time is considered since the edge deviation due to other types of uncertainty can be derived similarly.

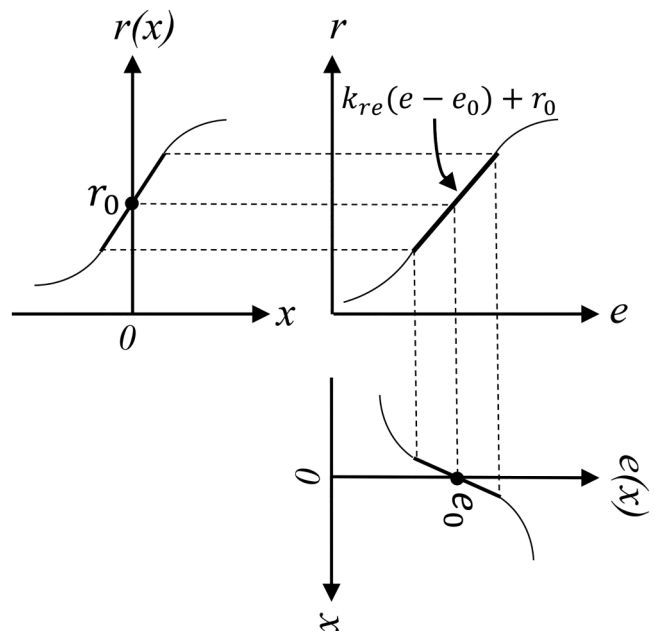


FIG. 5. Conversion of exposure $e(x)$ into developing rate $r(x)$ in the edge region can be done through a linear mapping of the e -to- r curve.

11 November 2024 17:00:23

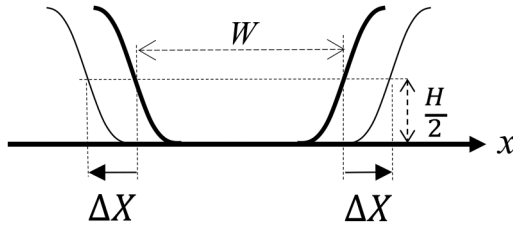


FIG. 6. The sidewall of the remaining resist profile for a feature with width W is illustrated. The width of a feature is measured at the middle layer of resist. When overdeveloped by ΔX on each side at the resist height of $\frac{H}{2}$, the width becomes $W + 2\Delta X$.

Let ΔT represent a fluctuation of developing time. Then, the actual developing time is $T_0 + \Delta T$. The deviation in the edge location from the target edge at $x = 0$ due to the fluctuation, denoted by ΔX , meets the following condition (see Fig. 7):

$$(k_r \Delta X + r_0)(T_0 + \Delta T) = \frac{H}{2}. \quad (10)$$

From Eq. (10),

$$\Delta X = \frac{r_0}{k_r} \left(\frac{1}{1 + \frac{\Delta T}{T_0}} - 1 \right). \quad (11)$$

Noting that $k_r = k_{re} k_e = k_{re} e'(0)$ and referring to Eq. (5),

$$\Delta X = \frac{r_0 \sqrt{\pi} (1 + \eta) \left(\frac{1}{1 + \frac{\Delta T}{T_0}} - 1 \right)}{k_{re} D_0 \left[\frac{1}{\alpha} \left(e^{-\frac{\Delta W^2}{\alpha^2}} - e^{-\frac{(W - \Delta W)^2}{\alpha^2}} \right) + \frac{\eta}{\beta} \left(e^{-\frac{\Delta W^2}{\beta^2}} - e^{-\frac{(W - \Delta W)^2}{\beta^2}} \right) \right]}. \quad (12)$$

In Eq. (12), r_0 is fixed since e_0 is maintained at the same level by adjusting D_0 , and k_{re} is determined by the resist type and developer. In this study, instead of examining the value of ΔX for a specific case of the e-beam lithographic process, the *normalized deviation* in the edge location (“normalized edge deviation” in

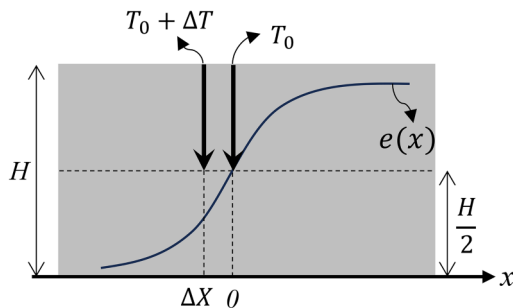


FIG. 7. Edge deviation caused by the variation in developing time where $\Delta T > 0$ and $\Delta X < 0$, i.e., the left edge is shifted to the left widening the feature width.

short) is considered for general cases since the main objective is to find the minimum deviation. In analyzing the edge deviation for a range of certain parameter, the normalized edge deviation is defined as $\frac{\Delta X}{\Delta X_{\min}}$, where ΔX_{\min} is the minimum value of ΔX in the range. The normalized edge deviation of 1 corresponds to the minimum deviation, i.e., when the edge location is most stable against the stochastic variation of the e-beam lithographic process.

V. ANALYSIS

The deviation in the edge location due to the variation in the developing time is affected by the lithographic and pattern parameters. In this section, to demonstrate the usefulness of the closed-form expression of the deviation derived in this study, the dependency of the deviation on each parameter is analyzed in terms of the normalized edge deviation. Note that this analysis can be done readily by evaluating ΔX in Eq. (12) with a parameter varied. The dependency is plotted for several cases where the resist thickness and developing rate at the feature edge are set to 200 nm and 100 nm/min, respectively. In each case, one parameter is varied with all the others fixed. In this section, “edge deviation” refers to the normalized edge deviation.

The dependency of the normalized edge deviation on the forward-scattering range α is shown for $1 \text{ nm} \leq \alpha \leq 5 \text{ nm}$ in Fig. 8. The edge deviation monotonically increases with α . For a larger α , i.e., a broader LSF, the exposure contrast over the feature edge is lower,¹² leading to a larger edge deviation. As α increases, the exposure level at the feature edge (e_0) decreases, and therefore, the dose needs to be increased to maintain e_0 at a fixed level (refer to Sec. IV A). Then, this increased exposure level would make the exposure contrast higher. However, this effect remains negligible until α becomes comparable to the feature width W .

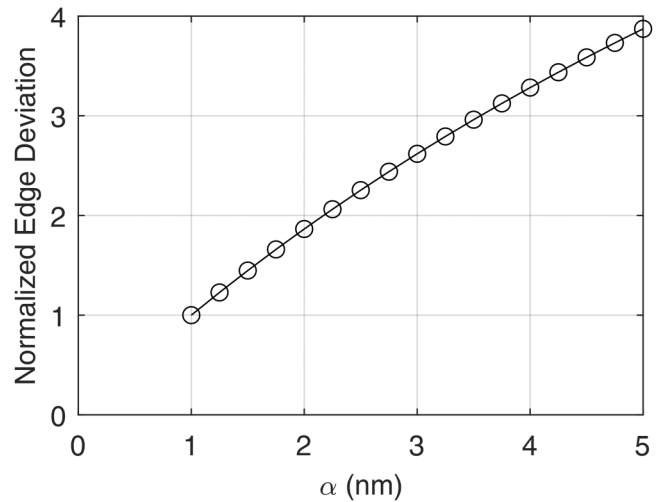


FIG. 8. Normalized edge deviation as a function of the forward-scattering range α when the developing time is increased by 5%, i.e., $\frac{\Delta T}{T_0} = 0.05$: $\beta = 10 \text{ nm}$, $\eta = 0.8$, $W = 20 \text{ nm}$, $\Delta W = 0 \text{ nm}$, $H = 200 \text{ nm}$, and $r_0 = 100 \text{ nm/min}$.

11 November 2024 17:00:23

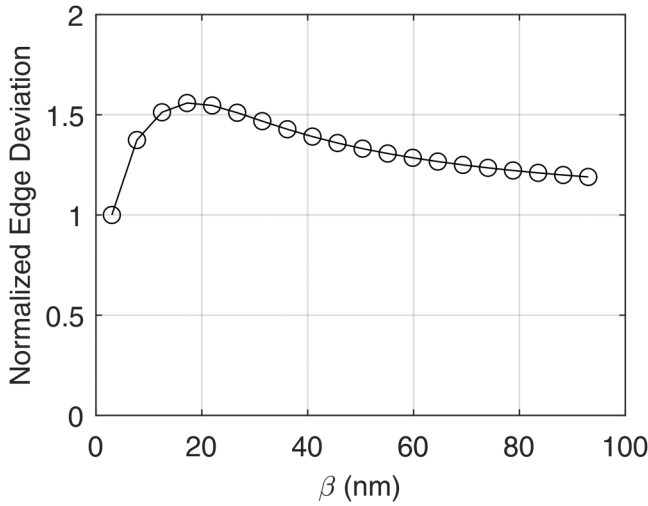


FIG. 9. Normalized edge deviation as a function of the backscattering range β when the developing time is increased by 5%, i.e., $\frac{\Delta T}{T_0} = 0.05$: $\alpha = 3$ nm, $\eta = 0.8$, $W = 20$ nm, $\Delta W = 0$ nm, $H = 200$ nm, and $r_0 = 100$ nm/min.

In Fig. 9, the dependency of the normalized edge deviation on the backscattering range β is plotted for $\beta \geq \alpha$. The edge deviation shows a bitonic behavior as β increases. The backscattering component of LSF has a broader distribution than the forward-scattering component (characterized by α), making the exposure contrast over the feature edge lower compared to the case where only the forward-scattering is considered (equivalently $\beta = \alpha$). As β increases

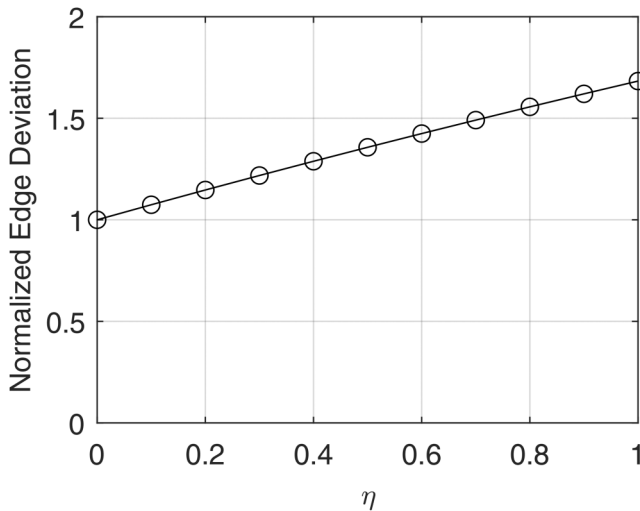


FIG. 10. Normalized edge deviation as a function of the ratio of the backscattered energy to the forward-scattered energy η when the developing time is increased by 5%, i.e., $\frac{\Delta T}{T_0} = 0.05$: $\alpha = 3$ nm, $\beta = 20$ nm, $W = 20$ nm, $\Delta W = 0$ nm, $H = 200$ nm, and $r_0 = 100$ nm/min.

starting from α , the exposure contrast quickly decreases due to the backscattering component where the decreasing rate becomes smaller for a larger β . Therefore, the edge deviation increases rapidly in the beginning and then the increase slows down. At the same time, the exposure contribution by the backscattering becomes smaller for a larger β . This makes e_0 lower so that the dose is increased, leading to a gradual increase in the exposure contrast and therefore a gradual decrease in the edge deviation as β continues to increase. Therefore, the overall behavior of the edge deviation becomes bitonic.

In Fig. 10, the ratio of the backscattered energy to the forward-scattered energy, η , is varied from 0 to 1 in examining the behavior of the normalized edge deviation. It is observed that the edge deviation linearly increases with η . As η increases, the relative effect of the

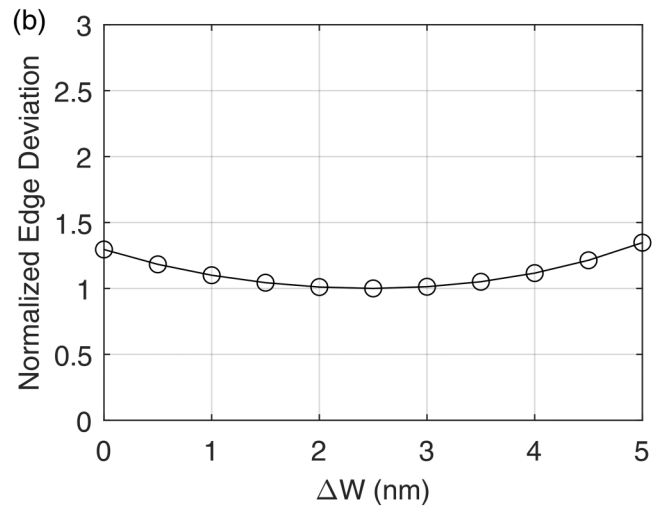
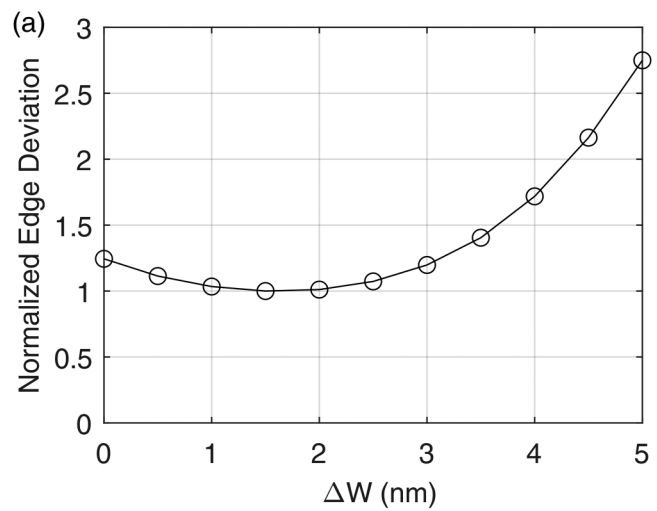


FIG. 11. Normalized edge deviation as a function of the feature-width reduction ΔW when the developing time is increased by 5%, i.e., $\frac{\Delta T}{T_0} = 0.05$, (a) $\alpha = 3$ nm and (b) $\alpha = 4$ nm: $\beta = 20$ nm, $\eta = 0.8$, $W = 20$ nm, $H = 200$ nm, and $r_0 = 100$ nm/min.

11 November 2024 17:00:23

backscattering on the exposure distribution increases. Since the backscattering component of exposure has a broader distribution, the exposure contrast decreases with η , and hence, the edge deviation increases.

In Fig. 11, the dependency of the normalized edge deviation on the reduction of feature width, ΔW , is examined in two different cases of α . As ΔW increases (with the dose fixed), the exposure contrast at the feature edge decreases slower in the beginning and then faster.¹² However, with the feature-width reduced, the dose needs to be increased to fully develop the feature in a typical PEC scheme or equivalently to maintain e_0 at a fixed level as mentioned earlier. The increase in exposure contrast due to the increased dose

is initially dominant, and the decrease caused by the feature-width reduction becomes more influential as the feature width is further reduced. Hence, as seen in Fig. 11, the edge deviation exhibits a bitonic behavior, i.e., decreases initially and then increases. For a smaller α (a sharper LSF), the fast decrease of exposure contrast (due to the reduction of feature width) starts at a smaller ΔW . This is the reason why ΔW for achieving the minimum deviation (normalized edge deviation of 1) is smaller for a smaller α [Fig. 11(a)] than for a larger α [Fig. 11(b)].

In Fig. 12, the normalized edge deviation is plotted as a function of the variation in the developing time. As expected, the edge deviation monotonically increases with the variation in both directions, i.e., T_0 increases [Fig. 12(a)] or decreases [Fig. 12(b)]. The reason why the two graphs in Fig. 12 are not completely symmetric with respect to $\Delta T = 0$ is that the relationship between the developing rate and time is not linear.

In Fig. 13, the dependency of the normalized edge deviation on feature width W is examined. When W is smaller than the forward-scattering range α , the exposure contrast and level at the feature edge are low. Though the dose is increased to compensate for the low exposure level (to maintain e_0), the exposure contrast is still low leading to a relatively high edge deviation. As W increases, the exposure contrast (without the dose compensation) increases, but the level of dose compensation (increase) is reduced. In the beginning, the effect of the decreasing dose compensation does not show up, and therefore, the edge deviation decreases. Beyond a certain point, the exposure contrast starts to decrease slightly mainly due to the fact that the dose compensation continues to be reduced, i.e., the edge deviation starts to increase slow but levels out close to 1.

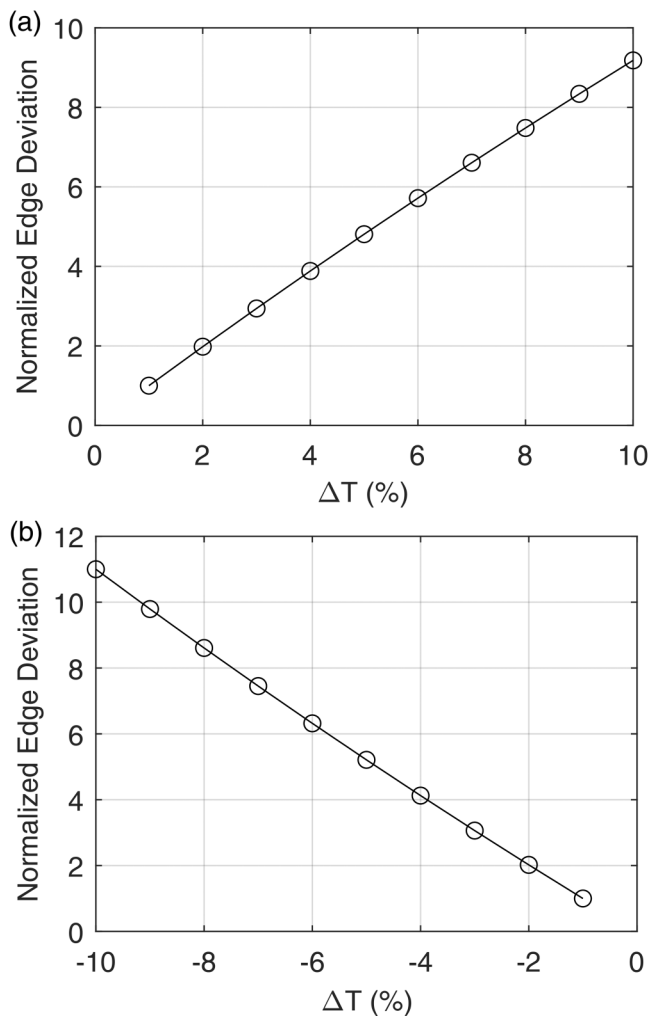


FIG. 12. Normalized edge deviation as a function of the percent variation in the developing time ΔT (a) when $\Delta T > 0$ and (b) when $\Delta T < 0$: $\alpha = 3$ nm, $\beta = 20$ nm, $\eta = 0.8$, $W = 20$ nm, $\Delta W = 0$ nm, $H = 200$ nm, and $r_0 = 100$ nm/min.

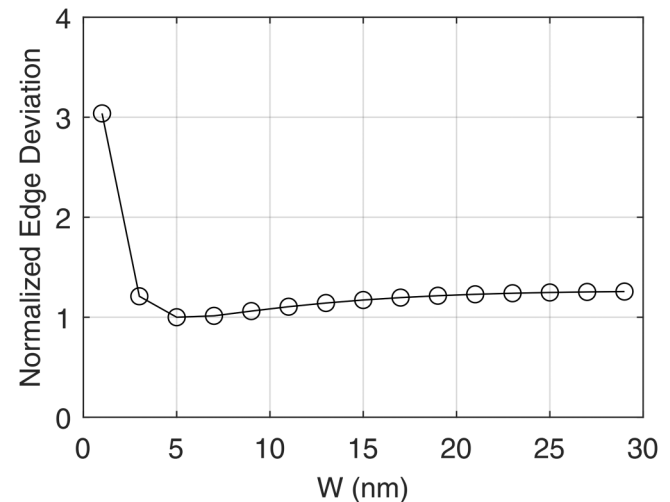


FIG. 13. Normalized edge deviation as a function of the feature width W when the developing time is increased by 5%, i.e., $\frac{\Delta T}{T_0} = 0.05$: $\alpha = 3$ nm, $\beta = 20$ nm, $\eta = 0.8$, $\Delta W = 0$ nm, $H = 200$ nm, and $r_0 = 100$ nm/min.

11 November 2024 17:00:23

VI. SUMMARY

As the feature size continues to decrease, the accuracy of realizing the CD as designed becomes increasingly important. The CD is determined by the locations of feature edges in the written pattern. The edge location can be deviated (from the target location or the location that would be achieved otherwise) due to the stochastic uncertainty in the lithographic process. In this study, a closed-form mathematical expression of the edge deviation has been derived in terms of the lithographic and pattern parameters in e-beam lithography. The mathematical expression enables one to analyze the dependency of the edge deviation on the lithographic and pattern parameters easily without resorting to simulation. Specifically, the expression of the normalized edge deviation aims at finding the optimal point where the deviation is minimal instead of computing the value of deviation.

In the derivation, it is assumed that the developing rate (equivalently exposure) varies linearly with X (when a rectangular feature such as lines is long in the Y dimension) but does not vary along the resist-depth dimension. These assumptions are justifiable since the stochastic uncertainty is of small scale so that the deviation of the feature edge would occur within a small edge region where the linearity and uniformity in the spatial distribution of developing rate hold.

While the double-Gaussian model of LSF (equivalently PSF) is employed in this study, the closed-form expression of edge deviation can be readily generalized for other models including an LSF in the numeric format.¹² Hence, the result of this study has a broad applicability.

The results reported in this paper may be referred to for not only examining the dependency of edge deviation on the lithographic and pattern parameters but also designing a PEC method that focuses on both accuracy and stability of feature-edge location and thereby improves the process latitude.

The future study may include relaxing the assumptions made in this study, e.g., taking into account the layer-dependent exposure, the lateral development of resist, etc.

AUTHOR DECLARATIONS

Conflict of Interest

The authors have no conflicts to disclose.

Author Contributions

Soo-Young Lee: Conceptualization (lead); Formal analysis (lead); Investigation (lead); Methodology (lead); Software (lead); Visualization (lead); Writing – original draft (lead).

DATA AVAILABILITY

The data that support the findings of this study are available within the article.

REFERENCES

- ¹C. Vieu, F. Carcenac, A. Pepin, Y. Chen, M. Mejias, A. Lebib, L. Manin-Ferlazzo, L. Courraud, and H. Launois, *Appl. Surf. Sci.* **164**, 111 (2000).
- ²M. Aktary, M. O. Jensen, K. L. Westra, M. J. Brett, and M. R. Freeman, *J. Vac. Sci. Technol. B* **21**, L5 (2003).
- ³B. Bilenberg, S. Jacobsen, M. S. Schmidt, L. H. D. Skjolding, P. Shi, P. Boggild, J. O. Tegenfeldt, and A. Kristensen, *Microelectron. Eng.* **83**, 1609 (2006).
- ⁴C. M. Kolodziej and H. Maynard, *Chem. Mater.* **24**, 774 (2012).
- ⁵A. Chaker, H. R. Alty, P. Tian, A. Kotsovinos, G. A. Timco, C. A. Muryn, S. M. Lewis, and R. E. P. Winpenny, *ACS Appl. Nano Mater.* **4**, 406 (2021).
- ⁶R. Rau, J. H. McClellan, and T. J. Drabik, *J. Vac. Sci. Technol. B* **14**, 2445 (1996).
- ⁷B. D. Cook and S.-Y. Lee, *IEEE Trans. Semicond. Manuf.* **11**, 117 (1998).
- ⁸M. Osawa, K. Takahashi, M. Sato, H. Arimoto, K. Ogino, H. Hoshino, and Y. Machida, *J. Vac. Sci. Technol. B* **19**, 2483 (2001).
- ⁹T. Klimpel, M. Schulz, R. Zimmermann, H.-J. Stock, and A. Zepka, *J. Vac. Sci. Technol. B* **29**, 06F315 (2011).
- ¹⁰Q. Dai, S.-Y. Lee, S.-H. Lee, B.-G. Kim, and H.-K. Cho, *J. Vac. Sci. Technol. B* **30**, 06F307 (2012).
- ¹¹S.-Y. Lee and B. D. Cook, *IEEE Trans. Semicond. Manuf.* **11**, 108 (1998).
- ¹²S.-Y. Lee, *J. Vac. Sci. Technol. B* **41**, 062606 (2023).
- ¹³Q. Dai, S.-Y. Lee, S.-H. Lee, B.-G. Kim, and J.-K. Cho, *Microelectron. Eng.* **88**, 3054 (2011).